Journal of Power Sources 195 (2010) 4313–4317

Contents lists available at ScienceDirect

Journal of Power Sources

journal homepage: www.elsevier.com/locate/jpowsour

High rate cycling performance of $Li_{1.05}Ni_{1/3}Co_{1/3}Mn_{1/3}O_2$ materials prepared by sol–gel and co-precipitation methods for lithium-ion batteries

R. Santhanam, B. Rambabu*

Solid State Ionics and Surface Sciences Lab, Department of Physics, Southern University and A&M College, Baton Rouge, LA 70813, USA

ARTICLE INFO

Article history:
Received 11 December 2009
Received in revised form 6 January 2010
Accepted 7 January 2010
Available online 13 January 2010

Keywords:
Lithium metal oxide
Sol–gel
Co-precipitation
High-rate
Lithium batteries

ABSTRACT

High rate performance of $Li_{1.05}Ni_{1/3}Co_{1/3}Mn_{1/3}O_2$ cathode materials prepared using sol–gel (SG) and co-precipitation (CP) methods were investigated. Scanning electron microscopy results showed that the particle sizes of the materials prepared by SG and CP methods were 300–400 nm and 1–2 μm, respectively. Rate capability tests were performed and compared on these cathode materials with same electrode loading (7 mg cm^{-2}). $Li_{1.05}Ni_{1/3}Co_{1/3}Mn_{1/3}O_2$ cathode with smaller particle size (SG-nano) demonstrated higher discharge capacity than that of the cathode with larger particle size (CP-micro) at different C-rates. However, upon extended cycling at 1C and 8C, CP-micro showed better capacity retention when compared to that of SG-nano. CP-micro exhibited 95 and 91% where as SG-nano exhibited only 87 and 76%, respectively, at 1C and 8C after 50 cycles. The results showed that the use of nanosized materials was advantageous for obtaining a better rate capability where as the use of microsized materials was beneficial for better capacity retention during extended cycling at high C-rates.

1. Introduction

Rechargeable lithium-ion battery has long been considered as an attractive power source for portable electronic devices such as notebook computers, cellular phones, and digital cameras. It has now been a prime candidate for hybrid electric vehicles (HEVs), plug-in hybrid electric vehicles (PHEVs) and electric vehicles (EVs) for reasons of high energy density, high power density, better cyclability and safety [1–4]. $LiCoO_2$ is the most widely used cathode material in commercial lithium-ion battery because it is reasonably easy to synthesize and has excellent electrochemical properties [5–7]. But due to its high cost and toxicity, an intensive research for new cathode materials have been underway to find alternatives in recent years [8–10]. Recently, manganese based layered compounds as cathode materials for lithium-ion batteries are of great interest and are potential candidates to replace the commercial $LiCoO_2$. These include $LiNi_{1/2}Mn_{1/2}O_2$ [3,11], $LiNi_{1/3}Co_{1/3}Mn_{1/3}O_2$ [12–15], and its derivatives such as $LiNi_xCo_{1-2x}Mn_xO_2$ ($0 \geq x \geq 1/3$) [16–18]. The electrochemical processes involve the redox pair of Ni^{2+}/Ni^{4+} with two-electron transfer in the series of these compounds. Among them, $LiNi_{1/3}Co_{1/3}Mn_{1/3}O_2$ has been studied extensively as promising cathode material for lithium-ion batteries as it exhibits much higher capacity, structural stability and enhanced safety [19,20].

Although, high voltage, portability, safety and excellent cyclability have contributed to the commercial success of lithium-ion rechargeable batteries, future applications, like HEV, PHEV require a higher charge–discharge rate capability. Rate capability limitations result from a number of factors including low ionic and electronic conductivity of the electrode materials and slow insertion/extraction of lithium ions into the cathode, at the cathode/electrolyte interface. The electrochemical performance of $LiNi_{1/3}Co_{1/3}Mn_{1/3}O_2$ materials used as cathode material in secondary lithium-ion batteries are strongly affected by their preparation processes. Therefore, selecting a synthetic method is important to obtain phase-pure and fine-sized $LiNi_{1/3}Co_{1/3}Mn_{1/3}O_2$ materials. Recently, a great deal of research has been focused on the preparation methods to enhance the electrochemical properties. $LiNi_{1/3}Co_{1/3}Mn_{1/3}O_2$ material is generally synthesized by solid state reaction, sol–gel process, and co-precipitation methods [20–24]. Very recently, microwave [25], self-propagating solid state metathesis [26], rheological phase [27], thermal polymerization [28] and microemulsion [29] methods have been used to synthesize and enhance the electrochemical properties of $LiNi_{1/3}Co_{1/3}Mn_{1/3}O_2$ materials. Recent trend in research and development of lithium batteries is to use nanosized cathode materials. The rate capability is expected to improve for nano materials due to higher the surface area for charge transfer and shorter diffusion length when compared to microparticles. However, the use of nano materials with a high surface area would have high surface reactivity and possible detrimental surface-side reactions, and poor inter-particle electrical contact. From electrochemical and spectroscopy measurements,

* Corresponding author. Tel.: +1 225 771 4130; fax: +1 225 771 2310.
E-mail address: rambabu@cox.net (B. Rambabu).

0378-7753/$ – see front matter © 2010 Elsevier B.V. All rights reserved.
doi:10.1016/j.jpowsour.2010.01.016

it has been reported that nanoparticles of spinel cathode material are much more reactive toward electrolyte species than microsized particles which results dissolution of metal ions from the nanosized particles [30].

Although a number studies focused on synthetic methods or electrochemical properties of as-prepared $LiNi_{1/3}Co_{1/3}Mn_{1/3}O_2$ material obtained from various temperatures, and systematic approach to show the high rate performance of material synthesized by different methods is limited. In spite of the fact that the electrode loading is an important factor to evaluate the differences in the high rate performance of the materials with different particle sizes, previous studies ignored this issue. When the electrochemical performances of different cathode materials are compared, loading is very important especially at high C-rates. For example, an electrode with higher loading would have higher thickness and at high C-rates, the resistance for lithium insertion and deinsertion will be relatively higher compared to that of the electrode with lower loading. Eventually, it would be hard to differentiate whether the performance is due to different loadings or different materials. Therefore, the loading should be the same for the materials with different particle size, especially, when we compare the high rate performance. Among the various methods used to synthesize cathode materials, sol–gel and co-precipitation methods are powerful, low cost and easy preparation methods for large scale production. High rate cyclability is an important factor to be studied for future application of lithium batteries for plug-in hybrid electric vehicles. Since the particle size of the materials prepared from SG and CP methods is different, the effect of particle size on the high rate performance of $Li_{1.05}Ni_{1/3}Co_{1/3}Mn_{1/3}O_2$ cathode with same loading (7 mg cm^{-2}), is investigated in the present work.

2. Experimental

2.1. Sol–gel (SG) method

$Li_{1.05}Ni_{1/3}Co_{1/3}Mn_{1/3}O_2$ cathode material was synthesized by the citric acid sol–gel method [31] in following manner. Stoichiometric amounts of $Li(CH_3COO)\cdot 2H_2O$, $Mn(CH_3COO)_2\cdot 4H_2O$, $Ni(CH_3COO)_2\cdot 4H_2O$, and $Co(CH_3COO)_2\cdot 4H_2O$ were dissolved in distilled water. Citric acid was used as a chelating agent. The solution pH was adjusted to 7.0 with ammonium hydroxide. The solution was heated at 70–80 °C until a transparent sol was obtained. The resulting gel precursor was dried at 120 °C for 4 h in air and followed with decomposition at 450 °C for 8 h to remove the organic contents. The decomposed powders were ground by ball milling (Spex 8000 Mixer/Mill) with stainless steel balls for 2 h and sintered at 850 °C in air for 12 h. The heating and cooling rates of the powder were 4 °C and 2 °C min^{-1}, respectively.

2.2. Co-precipitation (CP) method

$Li_{1.05}Ni_{1/3}Co_{1/3}Mn_{1/3}O_2$ cathode material was synthesized by co-precipitation method from Ni–Co–Mn mixed hydroxide precursor [17,24]. The precursor $(Ni_{1/3}Co_{1/3}Mn_{1/3})(OH)_2$ was prepared by dissolving stoichiometric amounts of $Ni(CH_3COO)_2\cdot 4H_2O$, $Co(CH_3COO)_2\cdot 4H_2O$ and $Mn(CH_3COO)_2\cdot 4H_2O$ in distilled water (cationic ratio of Ni:Co:Mn = 1:1:1) and the concentration of the total metal acetate was 2 mol L^{-1}. The aqueous solution was precipitated by adding LiOH (1 M)/NH_4OH (3 M) along with continued stirring. The solution was maintained at 50 °C for 24 h and the pH was controlled to 10–11. A green brown mixed hydroxide was precipitated. After filtering and washing, the hydroxide precipitate was dried at 120 °C for 24 h to remove the adsorbed water. Then, the obtained precursor was mixed with required amount of LiOH using a ball mill (Spex 8000 Mixer/Mill) and the powder was pressed into pellets. The pellets were initially heated to 400 °C for 6 h in air and then reground. Pellets were remade and subsequently sintered at 900 °C for 12 h in air in a muffle furnace. Heating up speed was fixed to 4 °C min^{-1} and cooling down speed was fixed to 2 °C min^{-1}.

2.3. Materials characterisation

The Li, Co, Ni and Mn contents in the resulting materials were analyzed using an inductively coupled plasma/atomic emission spectrometer (ICP/AES). The measured composition of the materials is close to the target composition so that the nominal compositions are used to describe the materials throughout this paper for simplicity. The phase purity was verified from powder X-ray diffraction (XRD) measurements. The particle morphology of the powders after sintering was obtained using a scanning electron microscopy (SEM). The charge and discharge characteristics of $Li_{1.05}Ni_{1/3}Co_{1/3}Mn_{1/3}O_2$ cathodes were examined in a CR2032 coin type half-cell. Cells were composed of a cathode and a lithium metal anode separated by a porous polypropylene separator (Celgard). Composite cathode was prepared by thoroughly mixing the active material (80%) with Super P carbon (10%) and polyvinylidene fluoride (10%) in N-methyl-pyrrolidinone. The slurry was then cast on aluminum foil and dried at 90 °C for 10 h in vacuum. The resulting electrode film was subsequently pressed and punched into a circular disc. The thickness and loading of the electrode film were 40 μm and 7.0 mg cm^{-2}, respectively. The electrolyte solution used was 1 M $LiPF_6$ in a mixture of ethylene carbonate–diethyl carbonate (1:1 volume, Ferro corporation, USA). The coin cell was assembled in an argon-filled glove box (Vacuum Atmospheres, USA). The cells were cycled at different C-rates between 2.5 and 4.3 V with an Arbin battery testing system.

3. Results and discussion

The XRD patterns of the $Li_{1.05}Ni_{1/3}Co_{1/3}Mn_{1/3}O_2$ material prepared by sol–gel and co-precipitation methods are presented in Fig. 1a and b, respectively. All the diffraction peaks can be indexed as a layered oxide structure based on a hexagonal α-$NaFeO_2$ structure. A small peak appeared around 2θ value 22° in Fig. 1a (not visible in Fig. 1b), might be due to the formation of Li_2MnO_3 due to a little excess lithium used in this work. The layered oxide structure has lithium ions at the 3a, the transition metal ions (Ni, Co, Mn) at 3b and oxygen ions at 6c sites. Since the ionic radii of Li^+ (0.76 Å) and Ni^{2+} (0.69 Å) ions are similar, a partial disordering among the 3a and 3b sites is expected and it is called as "cation-mixing" [32]. It has been established that the cation mixing deteriorates the electrochemical performance of the layered oxide materials. The integrated intensity ratio of the (0 0 3) to (1 0 4) lines (R) in the XRD patterns was shown to be a measurement of the cation mixing and a value of R <1.2 is an indication of undesirable cation mixing [32]. The ratio of the intensities of the (0 0 3) and (1 0 4) peaks are around 1.3 the materials prepared by both SG and CP methods, which indicate less cation disordering to deliver good electrochemical performance. The narrow diffraction peaks of the pattern indicate the high crystallinity of the prepared $Li_{1.05}Ni_{1/3}Co_{1/3}Mn_{1/3}O_2$ powder. In XRD patterns, the peak splits of 0 0 6/1 0 2 and 0 1 8/1 1 0 are known to be an indicator of layered structure such as $LiCoO_2$ and $LiNiO_2$ [33]. As can be seen in Fig. 1, clear peak splits of 0 0 6/1 0 2 and 1 0 8/1 1 0 are observed, which indicate the highly ordered layered structure of the prepared $Li_{1.05}Ni_{1/3}Co_{1/3}Mn_{1/3}O_2$ by SG and CP methods.

Scanning electron microscopy measurements were carried out to find out particle size, particle size distribution and morphology. Fig. 2a and b exhibit the scanning electron microscope (SEM) images of the $Li_{1.05}Ni_{1/3}Co_{1/3}Mn_{1/3}O_2$ materials prepared at 900 °C,

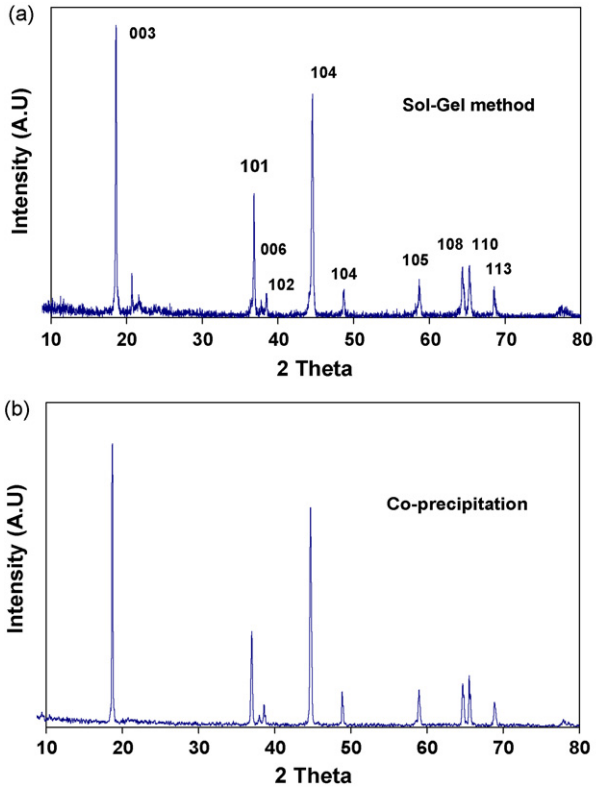

Fig. 1. XRD patterns of $Li_{1.05}Ni_{1/3}Co_{1/3}Mn_{1/3}O_2$ material prepared by (a) sol–gel, and (b) co-precipitation methods.

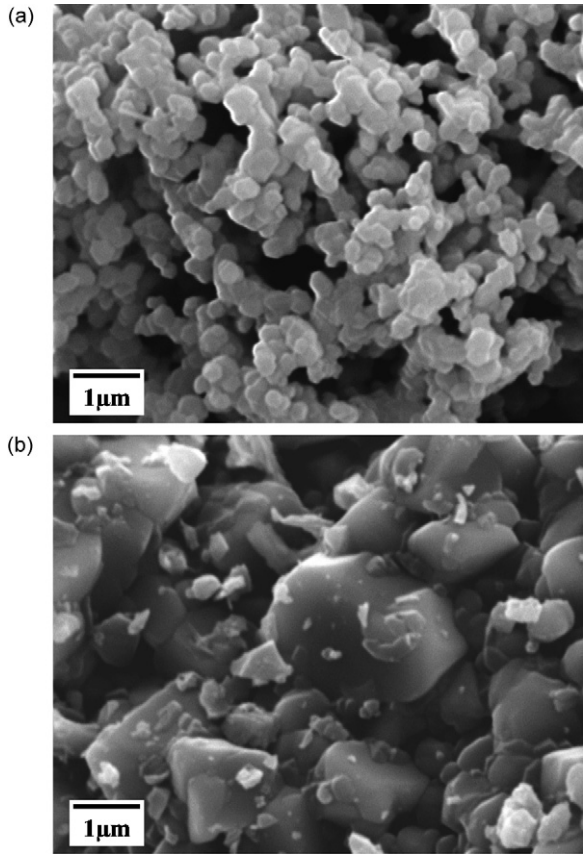

Fig. 2. SEM images of $Li_{1.05}Ni_{1/3}Co_{1/3}Mn_{1/3}O_2$ material prepared by (a) sol–gel, and (b) co-precipitation methods.

respectively, by SG and CP methods. $Li_{1.05}Ni_{1/3}Co_{1/3}Mn_{1/3}O_2$ material prepared by CP method show formation of larger particles in contrast to those prepared using SG method. The particle size distribution of the material prepared by SG method is relatively more uniform when compared to that of the material prepared by co-precipitation method. The size of the particle prepared by SG and CP methods is about 300–400 nm and 1–2 μm, respectively. The tap density depends on the shape and size of the particles. It has been reported that larger particles result in a higher tap density [34]. On all accounts, smaller size and good uniform particle size distribution of the $Li_{1.05}Ni_{1/3}Co_{1/3}Mn_{1/3}O_2$ material prepared by SG method result in a tap density of 1.7 g cm^{-3} and on the other hand, larger size and reasonable particle size distribution of the same material prepared by CP method result in a tap density of 2.2 g cm^{-3}.

In order to evaluate the effect of preparation method/particle size on the rate capability of $Li_{1.05}Ni_{1/3}Co_{1/3}Mn_{1/3}O_2$, the cells were cycled in the voltage range 2.5–4.3 V. Fig. 3 shows the discharge capacities of the SG- and CP- $Li_{1.05}Ni_{1/3}Co_{1/3}Mn_{1/3}O_2$/Li cells as a function of C-rate between 3.0 and 4.3 V vs Li. The cells were charged galvanostatically with a 0.1C-rate before each discharge testing, and then discharged at different C-rates from 0.1 to 8C-rates (16–1280 mAh g^{-1}). Clearly, the SG-$Li_{1.05}Ni_{1/3}Co_{1/3}Mn_{1/3}O_2$ delivered a higher discharge capacity than the CP- $Li_{1.05}Ni_{1/3}Co_{1/3}Mn_{1/3}O_2$, at all C-rates tested as shown in Table 1. For example, SG- and CP- $Li_{1.05}Ni_{1/3}Co_{1/3}Mn_{1/3}O_2$ cathodes delivered 168 mAh g^{-1} and 158 mAh g^{-1}, respectively, at 0.1C. At 8C-rate, the obtained discharge capacity of the SG-$Li_{1.05}Ni_{1/3}Co_{1/3}Mn_{1/3}O_2$ was about 133 mAh g^{-1}, while the CP-$Li_{1.05}Ni_{1/3}Co_{1/3}Mn_{1/3}O_2$ electrode showed discharge capacity of 124 at the same C-rate. Fig. 4 shows the cycling performance of $Li_{1.05}Ni_{1/3}Co_{1/3}Mn_{1/3}O_2$ cathode at different discharge rates (0.1C, 1C, 4C, 8C) between 2.5 and 4.3 V. The rate was increased from

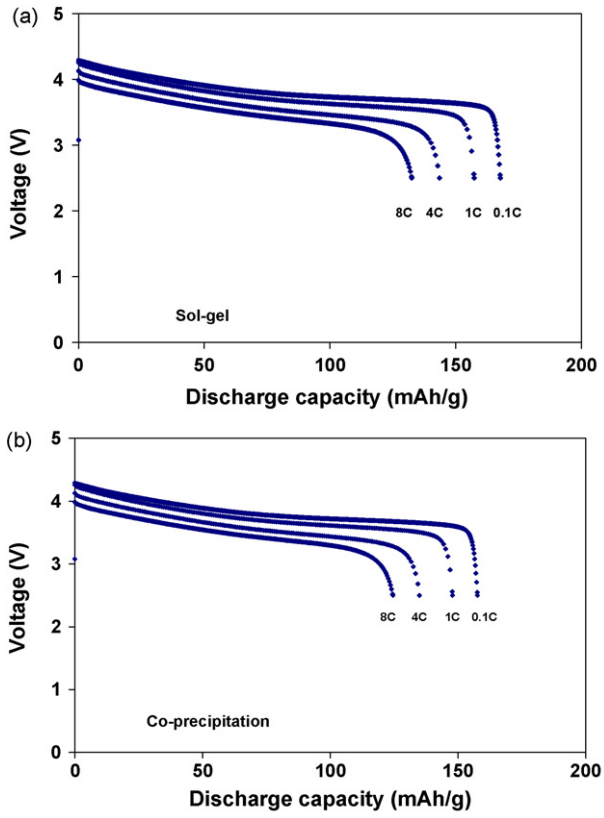

Fig. 3. Initial discharge curves of $Li_{1.05}Ni_{1/3}Co_{1/3}Mn_{1/3}O_2$ electrode prepared by (a) sol–gel, and (b) co-precipitation methods, at different C-rates, 0.1, 1, 4, 8C between 2.5 and 4.3 V.

Table 1
Discharge capacities of the $Li_{1.05}Ni_{1/3}Co_{1/3}Mn_{1/3}O_2$ cathode material prepared by sol–gel and co-precipitation methods at different C-rates.

C-rate	Discharge capacity of $Li_{1.05}Ni_{1/3}Co_{1/3}Mn_{1/3}O_2$, mAh g^{-1}	
	Sol–gel	Co-precipitation
0.1C	168	158
1.0C	158	148
5.0C	144	135
8.0C	133	124

0.1 to 8C stepwise, and finally returned to 0.1C. The sample SG-$Li_{1.05}Ni_{1/3}Co_{1/3}Mn_{1/3}O_2$ shows higher discharge capacity than CP-$Li_{1.05}Ni_{1/3}Co_{1/3}Mn_{1/3}O_2$ sample. The higher discharge capacity of SG- $Li_{1.05}Ni_{1/3}Co_{1/3}Mn_{1/3}O_2$ cathode, when compared to that of CP- $Li_{1.05}Ni_{1/3}Co_{1/3}Mn_{1/3}O_2$, was caused by shorter diffusion length (compare Fig. 3a and b) resulting from nanosized particles. The particle size plays an important role on the lithium storage performance. The obtained results thus strongly support that SG method is an effective method to prepare cathode material with higher capacity and rate capability.

In order to observe the effect of preparation method/particle size on cycling properties at high C-rates, SG- and CP-$Li_{1.05}Ni_{1/3}Co_{1/3}Mn_{1/3}O_2$/Li cells were assembled and the performance was measured at 1 and 8C-rates between 2.5 and 4.3 V. Fig. 5a and b indicates that the cycling performance of HG- and BM-$Li_{1.02}Ni_{0.4}Co_{0.2}Mn_{0.4}O_2$ electrode materials cycled at a high current rate of 1 and 8C, respectively. After 50 charge–discharge cycles at 1C, the CP- $Li_{1.05}Ni_{1/3}Co_{1/3}Mn_{1/3}O_2$ electrode exhibits excellent cycling performance with capacity retention ratio of about 95% when compared to that of SG- $Li_{1.05}Ni_{1/3}Co_{1/3}Mn_{1/3}O_2$ electrode which shows only 87% capacity retention ratio (Fig. 5a). Similarly, after 50 cycles at 8C cycling, SG- $Li_{1.05}Ni_{1/3}Co_{1/3}Mn_{1/3}O_2$ cathode exhibited relatively poor capacity retention (76%) than that of CP-$Li_{1.05}Ni_{1/3}Co_{1/3}Mn_{1/3}O_2$ (91%) as shown in Fig. 5b. The obtained cycling results thus support CP method to prepare material with excellent cyclability. The CP-micro $Li_{1.05}Ni_{1/3}Co_{1/3}Mn_{1/3}O_2$ cathode exhibits good cycle performance even at high discharge rates, indicating possibility as a candidate of cathode material for lithium-ion batteries.

To provide more information about the difference in electrochemical performances of the nano and micro particles, impedance measurements were carried out on SG-nano $Li_{1.05}Ni_{1/3}Co_{1/3}Mn_{1/3}O_2$ cathode CP-micro $Li_{1.05}Ni_{1/3}Co_{1/3}Mn_{1/3}O_2$ cathode after 50 cycles at 8C and the corresponding impedance plots are presented in Fig. 6. As shown in this figure, one can see the

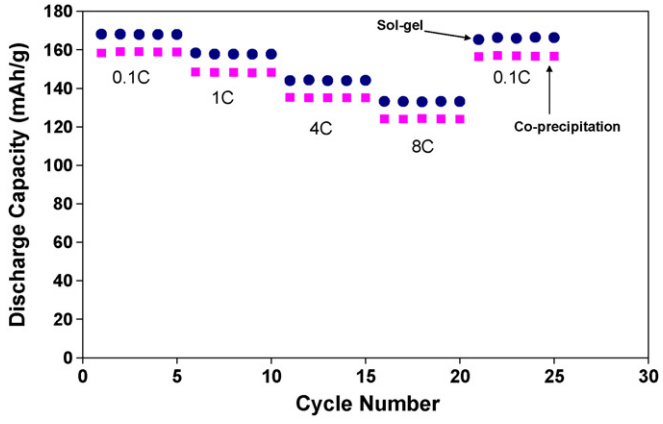

Fig. 4. Cycle performance of $Li_{1.05}Ni_{1/3}Co_{1/3}Mn_{1/3}O_2$ electrode prepared by (a) sol–gel, and (b) co-precipitation methods, at different discharge rates, 0.1, 1, 4, 8 C in the voltage range between 2.5 and 4.3 V.

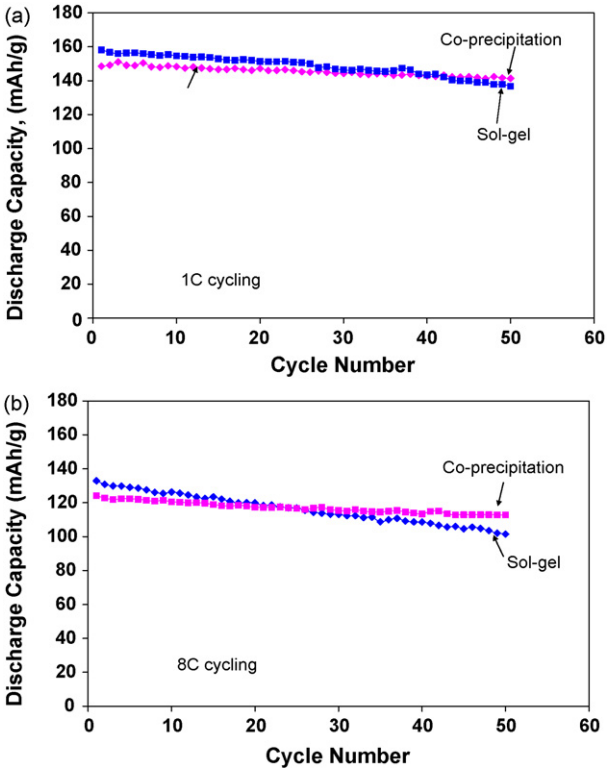

Fig. 5. High discharge rate cycling performance of $Li_{1.05}Ni_{1/3}Co_{1/3}Mn_{1/3}O_2$ electrode prepared by sol–gel, and co-precipitation methods, at (a) 1C, and (b) 8C in the voltage range between 2.5 and 4.3 V.

difference in interface impedance. The charge transfer resistance of SG-nano $Li_{1.05}Ni_{1/3}Co_{1/3}Mn_{1/3}O_2$ cathode is 1.5 times higher than that of CP-micro $Li_{1.05}Ni_{1/3}Co_{1/3}Mn_{1/3}O_2$ cathode. From this result, it is evidenced that the increased surface area of the nanoparticles compared to that of microparticles, increases the insulating film formation due to increased decomposition reactions with the electrolyte during cycling. This insulating surface film would block the direct interconnections between the active particles and the electrolyte, and this would deteriorate the charge transfer reactions between the active particles and the current collector, causing an increase in charge transfer resistance.

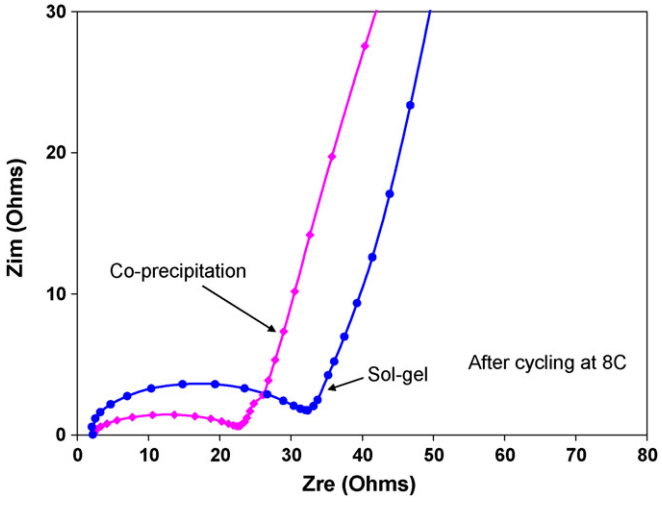

Fig. 6. Impedance plots of $Li_{1.05}Ni_{1/3}Co_{1/3}Mn_{1/3}O_2$ cathode prepared by sol–gel and co-precipitation methods after cycling at 8C.

Overall, the layered $Li_{1.05}Ni_{1/3}Co_{1/3}Mn_{1/3}O_2$ material prepared by SG method exhibited higher capacity and rate capability than that of material obtained by CP method. However, after 50 charge–discharge cycles at high C-rates, the cycling performance of the same material prepared by CP method showed higher capacity retention than that of the material obtained by SG method. The difference between the material prepared by SG and CP methods is the particle size. As seen from SEM images, the materials prepared by SG and CP methods have nanosized (300–400 nm) and microsized particles (1–2 μm), respectively. The surface reactions of both nano and micro particles of battery oxide materials are similar which involves the reaction between the solvent, for example ethylene carbonate (EC), and the oxygen on the surface of the material [30]. The reduced dimension of the particles significantly increases the lithium insertion and deinsertion due to short diffusion length for lithium-ion transport within the particles. However, at the same time, an increased surface area results in increased side reactions with the electrolyte and thus forming thicker surface film (solid electrolyte interface, SEI). It has been reported that the thickness of the surface film increased with increasing surface area of the cathode material and this film consisted of mostly organic $ROCO_2Li$ and ROLi products [35]. The thicker surface film would interfere badly with electrical contact between the particles during cycling and thus increasing capacity fading. It is known that commercial $LiPF_6$-based lithium battery electrolytes always contain a trace amount of water. It has been established that the $LiPF_6$ can be reacted with traces of water and produce a very reactive HF species. As a result, nanoparticles proceeds with Ni/Co/Mn metal dissolution. For microparticles, due to relatively lower surface area, the metal dissolution is limited and the thickness of the SEI film is also relatively lower. Thus, electrodes comprising microparticles show better capacity retention, during extended cycling, than electrodes comprising nanoparticles. Moreover, as mentioned earlier, the $Li_{1.05}Ni_{1/3}Co_{1/3}Mn_{1/3}O_2$ material prepared by CP method has higher tap density than that of the material prepared by SG method. The higher tap density results in higher volumetric energy density. High volumetric energy density is desirable for the active material in practical lithium-ion batteries. Therefore, the high tap density together with good high rate cycling performance of the prepared $Li_{1.05}Ni_{1/3}Co_{1/3}Mn_{1/3}O_2$ material by CP method make it a promising alternative to next generation lithium-ion batteries.

4. Conclusions

The study reported herein demonstrates and compares the high rate performance of the layered $Li_{1.05}Ni_{1/3}Co_{1/3}Mn_{1/3}O_2$ material prepared by sol–gel and co-precipitation method. Since the particle sizes of the cathode materials obtained by these methods were different, the effect of particle size on the electrochemical properties was investigated in detail. The $Li_{1.05}Ni_{1/3}Co_{1/3}Mn_{1/3}O_2$ electrode comprising nanoparticles (SG-nano) delivered a higher capacity at higher C-rates than electrode comprising microparticles (CP-micro) due to shorter diffusion length and higher surface area. However, CP-mico showed better capacity retention than SG-nano at high C-rates (1C and 8C) during extended cycling due to lower surface area and hence decreased side reactions with the electrolyte. From the results obtained from this work, it can be concluded that the layered $Li_{1.05}Ni_{1/3}Co_{1/3}Mn_{1/3}O_2$ cathode prepared by CP method which gave excellent capacity retention in high rate cycling and favoring the future use of this cathode material for high power applications.

Acknowledgements

This work is supported by U.S-DOD-ARO-Electrochemistry and Advanced Energy Conversion Division under the grant # W911NF-08-C-0415 (Proposal No: 52322-CH-H (BOBBA)). BRB and R. Santhanam thank Dr. Robert Mantz for supporting cathode materials research for developing hybrid energy storage devices.

References

[1] J.M. Tarascon, M. Armond, Nature 414 (2001) 359.
[2] M.S. Whittingham, Chem. Rev. 104 (2004) 4271.
[3] K.S. Kang, Y.S. Meng, J. Breger, C.P. Grey, G. Ceder, Science 311 (2006) 977.
[4] P.G. Bruce, B. Scrosati, J.M. Tarascon, Angew. Chem. Int. Ed. 47 (2008) 2930.
[5] J.S. Bok, J.H. Lee, B.K. Lee, Solid State Ionics 169 (2004) 139.
[6] M. Okubo, E. Hosono, J. Kim, M. Enomoto, N. Kojima, T. Kudo, H. Zhou, I. Honma, J. Am. Chem. Soc. 129 (2007) 7444.
[7] H. Chen, X. Qiu, W. Zhu, P. Hagenmuller, Electrochem. Commun. 4 (2002) 488.
[8] Y. Chen, G.X. Wang, K. Konstantinov, H.K. Liu, S.X. Dou, J. Power Sources 119–121 (2003) 184.
[9] B.J. Hwang, Y.W. Tsai, C.H. Chen, R. Santhanam, J. Mater. Chem. 13 (2003) 1962.
[10] A.V. Murugan, T. Muraliganth, A. Manthiram, J. Phys. Chem. C 112 (2008) 14665.
[11] B.J. Hwang, T.H. Yu, M.Y. Cheng, R. Santhanam, J. Mater. Chem. 19 (2009) 4536.
[12] T. Ohzuku, Y. Makimura, Chem. Lett. (2001) 642.
[13] J. Cho, A. Manthiram, J. Electrochem. Soc. 152 (2005) A1714.
[14] B.J. Hwang, Y.W. Tsai, D. Cariler, G. Ceder, Chem. Mater. 15 (2003) 376.
[15] Y.W. Tsai, B.J. Hwang, G. Ceder, H.S. Sheu, D.G. Liu, J.F. Lee, Chem. Mater. 17 (2005) 3191.
[16] S.H. Park, C.S. Yoon, S.G. Kang, H.S. Kim, S.I. Moon, Y.K. Sun, Electrochim. Acta 49 (2004) 557.
[17] W.S. Yoon, Y. Paik, X.Q. Yang, M. Balasubramanian, J. McBreen, C.P. Grey, Electrochem. Solid-State Lett. 5 (2002) A263.
[18] S.W. Oh, S.H. Park, C.W. Park, Y.K. Sun, Solid State Ionics 171 (2004) 167.
[19] Y. Koyama, I. Tanaka, T. Ohuzuku, J. Power Sources 119–121 (2003) 644.
[20] J.M. Kim, H.T. Chung, Electrochim. Acta 49 (2004) 937.
[21] J. Guo, L. Jiao, H. Yuan, H. Li, M. Zhang, Y. Wang, Electrochim. Acta 51 (2006) 3731.
[22] D. Li, T. Muta, L. Zhang, M. Yoshio, H. Noguchi, J. Power Sources 132 (2004) 150.
[23] S.K. Hu, G.H. Cheng, M.Y. Cheng, B.J. Hwang, R. Santhanam, J. Power Sources 188 (2009) 564.
[24] B.C. Park, H.J. Bang, C.S. Yoon, S.T. Myung, J. Prakash, Y.K. Sun, J. Electrochem. Soc. 154 (2007) A520.
[25] B.J. Shen, J.S. Ma, H.C. Wu, C.H. Lu, Mater. Lett. 62 (2008) 4075.
[26] Y.S. He, Z.F. Ma, X.Z. Lia, Y. Jiang, J. Power Sources 163 (2007) 1053.
[27] H. Ren, Y. Wang, D. Li, L. Ren, Z. Peng, Y. Zhou, J. Power Sources 178 (2008) 439.
[28] C.X. Ding, Q.S. Meng, L. Wang, C.H. Chen, Mater. Res. Bull. 44 (2009) 492.
[29] C.H. Lu, Y.K. Lin, J. Power Sources 189 (2009) 40.
[30] Y. Talyosef, B. Markovsky, R. Lavi, G. Salitra, D. Aurbach, D. Kovacheva, M. Gorova, E. Zhecheva, R. Stoyanova, J. Electrochem. Soc. 154 (2007) A682.
[31] B.J. Hwang, R. Santhanam, D.G. Liu, J. Power Sources 97–98 (2001) 443.
[32] Z. Chen, J.R. Dahn, Electrochem. Solid-State Lett. 5 (2002) A213.
[33] Y. Gao, M.V. Yakovleva, W.B. Ebner, Electrochem. Solid-State Lett. 1 (1998) 117.
[34] J. Jouanneau, K.W. Ekerman, L.J. Krause, J.R. Dahn, J. Electrochem. Soc. 150 (2003) A1637.
[35] N. Liu, H. Li, Z. Wang, X. Huang, L. Chen, Electrochem. Solid-State Lett. 9 (2006) A328.